Available online at www.sciencedirect.com
SCIENCE DIRECT®
ELSEVIER
Earth and Planetary Science Letters 214 (2003) 515–528
EPSL
www.elsevier.com/locate/epsl

High-rate flexure of the East Greenland volcanic margin: constraints from $^{40}Ar/^{39}Ar$ dating of basaltic dykes☆

Xavier Lenoir [a,b,*], Gilbert Féraud [c], Laurent Geoffroy [b]

[a] *Laboratoire: Pétrologie, Modélisation des Matériaux et Processus, Tour 26/16, cc 110, Université Pierre et Marie Curie, 4 Place Jussieu, 75252 Paris Cedex 05, France*

[b] *Laboratoire de Géodynamique des Rifts et des Marges Passives, EA3264, Université du Maine, avenue Olivier Messiaen, 72805 Le Mans Cedex 09, France*

[c] *Géosciences Azur, UMR6526, CNRS and Université de Nice-Sophia Antipolis, Parc Valrose, 06108 Nice Cedex 02, France*

Received 19 November 2002; received in revised form 20 June 2003; accepted 14 July 2003

Abstract

In the North Atlantic domain, the SE Greenland volcanic margin developed in response to continental break-up at 57–54 Ma. Progressive tilting and intrusion of dykes reflect a major tectonic seaward-dipping flexing of the continental crust. We report eight new ages of tilted (pre-flexure) and vertical (post-flexure) dykes, determined by $^{40}Ar/^{39}Ar$ incremental heating experiments. Despite strong excess argon on plagioclase, measured $^{40}Ar/^{39}Ar$ plateau and mini-plateau ages of dykes from detailed step-heating experiments on mineral separates appear reliable and a systematic difference of ages is found between tilted and vertical dykes. In both studied areas – Kap Wandel (66°20′N) and Kap Gustav Holm (66°40′N) – tilted dykes show ages of ~54–55 Ma whereas vertical dykes are younger with ages of ~51 Ma. Therefore, it appears that the crustal flexing of the volcanic passive margin is a short-duration event (< 2.9 Ma). These new dates and estimates of finite extensional strain in the studied areas suggest a lower boundary for extensional strain rates as high as $7 \pm 2 \times 10^{-15}$ s^{-1}. This value is, however, a clear underestimation as it is difficult to estimate the full finite extension in the studied area. It suggests that the continental lithosphere at volcanic passive margins is softened by high thermal gradients.

Keywords: dykes; Ar-40/Ar-39 dating; Greenland; flexure; volcanic margin

1. Introduction

Volcanic passive margins (VPMs) are associated with the extrusion and intrusion of large volumes of magma (e.g. [1,2]). The magmatism includes: (1) continental flood basalts covering large surfaces that predate plate break-up and (2) melting products associated geographically and temporally with plate break-up [3,4]. These break-up products include: (1) thick sequences of lava flows

* Corresponding author. 5 chemin Abbé de Born, 48100 Marvejols, France..
E-mail address: lenoir.xavier@free.fr (X. Lenoir).

☆ Supplementary data associated with this article can be found at doi:10.1016/S0012-821X(03)00392-3

0012-821X/03/$ – see front matter © 2003 Elsevier B.V. All rights reserved.
doi:10.1016/S0012-821X(03)00392-3

and tuffs constituting seaward-dipping reflector series (SDRS [5]) that may partially be exposed onshore [6,7] and which are fed by (2) coast-parallel dyke swarms and central intrusions and (3) postulated highly mafic magma underplated at Moho level (e.g. [8]). According to most authors, this voluminous magmatism during break-up is associated with a thermally anomalous mantle predating and accompanying plate break-up [1,9–11].

One of the more striking aspects of VPMs is the existence of a major crustal-scale seaward-dipping flexure of the margin. This flexure is expressed by lava flows in SDRS showing increase of dip with depth and progressive tilting of dykes feeding SDRS towards the ocean (e.g. [7,12–15]). Seaward-dipping lavas at SDRS have formerly been interpreted in Iceland as a progressive elastic flexion of the lithosphere beneath the increasing-with-time weight of the lava piles [16]. This gravitational interpretation did not take into account a possible dynamic stretching of the lithosphere. However, that the origin of these upper-crustal flexures is associated with the stretching of the lithosphere is now strongly suggested at VPMs from, notably, structural studies [6,7,14,15]. Syn-tectonic and syn-magmatic development of these upper-crustal flexures, which resemble syn-magmatic roll-over anticlines, is shown by the fan-like geometry of the lava piles controlled by continentward-dipping normal faults (e.g. [6,7,14]). Therefore, at VPMs, crustal extension results from both plumbing of the crust by dyke swarms (magmatic dilatation) and tectonic extension undertaken by continentward-dipping faults.

Assuming that seaward-dipping flexures at VPMs are the crustal expression of lithosphere stretching, the aim of this paper is to estimate the rate of crustal extension from geochronology of a VPM flexing. The average rate of crustal extension is the ratio between finite extension and duration of stretching (i.e. margin flexing). High rates of crustal extension have been suspected at VPMs from the widespread occurrence of pseudotachylytes (e.g. [17]). More precisely, the age and duration of crustal flexure at VPMs can be estimated in two ways: (1) dating the duration of syn-tectonic basalt flow extrusion in SDRS or exposed seaward-dipping basalts or (2) dating the duration of dyke emplacement, i.e. determining the precise time span between dykes injected in the earliest steps of crustal flexing and dykes injected when the flexing was just finished.

To estimate the average strain rate at a VPM, the volcanic margin of East Greenland is probably the best example. Indeed, the East Greenland Tertiary VPM is well exposed because of the uplift caused by the passage of the Iceland hotspot beneath the margin and recent isostatic rebound from glacial erosion (e.g. [18] and references herein). This paper focuses on the Coastal Dyke Swarm (CDS) which crops out in the eroded margin of SE Greenland (south of Kangerlussuaq area; Fig. 1) because this area has a relatively simple tectonic history during plate break-up in the North Atlantic domain [19]. The CDS corresponds to the most internal part of the margin which continues offshore.

Nearly only K/Ar ages are available for dykes [20] and published recent $^{40}Ar/^{39}Ar$ ages concern mainly flood basalts [21–24] and mafic intrusions [25–27] (see Table 1). K/Ar ages show a large dispersion as the result of alteration and variable amounts of excess ^{40}Ar [20] which is also shown by some recent $^{40}Ar/^{39}Ar$ measurements on dykes and sills [27]. In this view, the interval age of flexure at 50–52 Ma as proposed by Noble et al. [20] should be strengthened. Schwarz et al. [28] proposed that flexure occurs in a time interval of 250 kyr on the basis of a probable cooling history for the Skaergaard intrusion. However, no dating supports this time interval which is strongly dependent on estimates of many factors such as cooling rates, temperature distribution and latent heat. For these reasons, we performed detailed $^{40}Ar/^{39}Ar$ geochronology on basaltic dykes with the aim of determining the age and duration of coastal flexure. Bracketing in time the crustal flexure provides an estimate of strain rates in the internal part of the East Greenland VPM with major implications for crustal rheology during break-up over a thermal anomaly.

2. CDS of East Greenland

The CDS is well exposed on land along 350 km

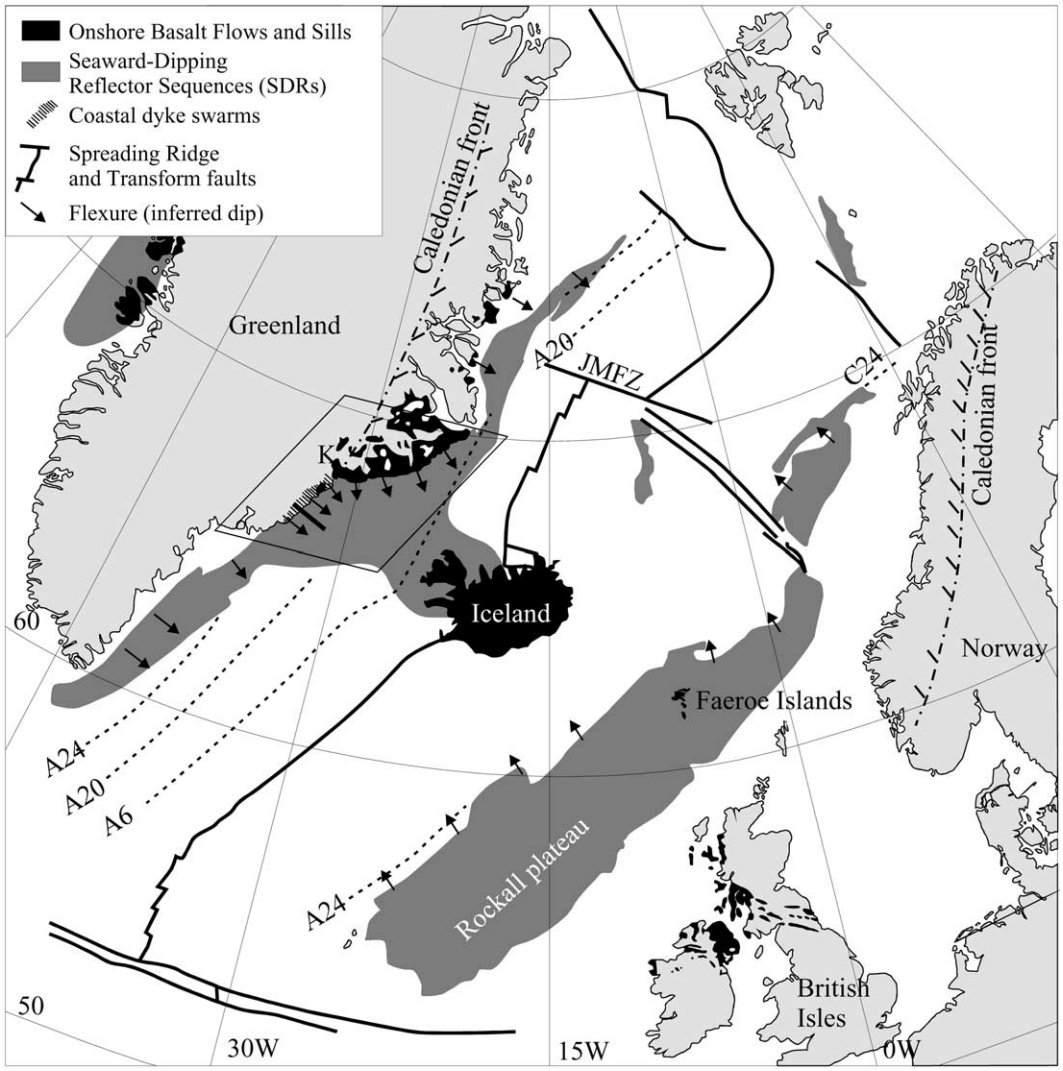

Fig. 1. Localization of the break-up axis, and distribution of seaward-dipping reflector sequences, continental flood basalts and CDSs in the North Atlantic domain. The inferred continent/oceanic boundary lies at the transition between flood basalts with landward structure and SDRs. Selected seafloor-spreading anomalies are shown by dashed lines. The thick straight line locates the schematic cross-section across the margin shown in Fig. 2. K = Kangerlussuaq; JMFZ = Jan Mayen Fracture Zone. After Larsen and Saunders [57].

of the uplifted coast of East Greenland, particularly between Kap Wandel, Nigertuluk and Kangerlussuaq (Fig. 2) where thick lava piles of continental flood basalt have been removed by erosion (>3 km [29]). The CDS trends approximately SW–NE for 250 km southwest of Kangerlussuaq, and E–W for 100 km to the east. These two branches of the CDS and a minor dyke swarm parallel to Kangerlussuaq fjord have been described as a triple rift junction [15,30]. The SW–NE branch of the CDS is subdivided into two major en échelon segments (100 km in length) which are separated by a large sinistral offset at Kruuse Fjord intrusion [13,31]. Minor subdivisions of the CDS occur at a smaller scale (few tens of kilometers) in both branches. These

Table 1
Summary of published recent $^{40}Ar/^{39}Ar$ ages on mafic intrusions and lavas

Magmatic structure	Locality	$^{40}Ar/^{39}Ar$ age (Ma)	Ref.
Mafic intrusions	Skaergaard	55.65 to 55.75 ± 0.3	[25]
	Imilik, intrusion II	56.2 ± 0.6	[27]
	Imilik, intrusion III	49.2 ± 0.2; 49.8 ± 0.2	[27]
	Lilloise	50.0 ± 0.4	[27]
	Kap Edward Holm	48.8 ± 0.2; 49.4 ± 0.2	[26,27]
	Nodre Aputitêp	48.0 ± 0.2	[26]
	Kruuse Fjord	48.0 ± 1.2	[27]
	Igtutarajik	47.0 ± 0.2	[27]
Sill complex	Sorgenfri Gletscher	56.0 ± 0.4; 56.3 ± 0.9	[27]
Onshore lavas	Scoreby Sund	54.5 ± 4.1 to 57.8 ± 4.5	[21]
	Blosseville Kyss	around 59–60 (lower series)	[23]
		around 54–57 (middle series)	[23]
	Igertiva	around 49.0–47.9	[27]
SDRs	Leg 152, Hole 917	60.1 ± 0.8 to 62.3 ± 1.4	[22]
	Leg 152, Hole 918	51.9 ± 0.8	[22]
	Leg 163, Hole 989B	57.1 ± 1.3	[24]
	Leg 163, Hole 989A	55.6 ± 0.6 and 55.8 ± 0.7	[24]
	Leg 163, Hole 988	49.6 ± 0.2	[24]

Errors are at the 1σ level, except for [22,25] (2σ).

latter structures correspond to the second- and third-order segmentation of the East Greenland margin, respectively [15].

The internal structure of the CDS appears to have been constructed by multiple generations of partially overlapping, laterally discontinuous swarms [13,31]. In general, dykes are roughly parallel to the coast although older dykes have a more easterly strike than younger dykes [31]. Older dykes dip landward as a result of the seaward flexing of the crust [14,15]. The flexure is well marked by the seaward increase in tilting of the dykes. Younger cross-cutting dykes also dip landward but much more steeply or are vertical [15,31]. Therefore, the CDS presents an asymmetric fanning geometry in cross-section. Younger dykes are generally thinner than older dykes and their density increases toward the sea [13,31].

Petrological and geochemical studies of the CDS in the Kangerlussuaq area [32,33] and in the southern part of the dyke swarm [34] have shown that dyke intrusion records a wide spectrum of magmatic compositions from tholeiites and picrites to transitional and alkalic varieties. Older, tilted (pre-flexure) dykes are mainly picrites and tholeiites whereas younger, near-vertical (post-flexure) dykes have transitional-tholeiitic and alkaline compositions [31,32,34]. Only K/Ar ages of basalts from CDS in the Kangerlussuaq area have been published previously [20]. The results show a large dispersion of K/Ar ages from 35 to 300 Ma suggesting that the oldest ages are due to excess argon. Nevertheless, by tentatively selecting valid ages (apparently not affected by excess argon), Noble et al. [20] proposed that pre-flexure and post-flexure dykes were intruded between 51 and 53 Ma, and 49 and 51 Ma, respectively, and that the flexure formed around the interval 52–50 Ma.

3. Sampling and analytical procedure

We sampled 12 pairs of basaltic dykes along profiles across the margin in the southern part of CDS at Kap Wandel and Kap Gustav Holm (Fig. 2). Each pair of dykes is composed of one tilted dyke and one cross-cutting vertical dyke with the angular difference of dip ranging from 25 to 45° (Fig. 3A). This sampling estimates the local duration and the rate of flexing. We assume that pre- or syn-flexure dykes were intruded subvertically and progressively tilted during flexing. In this scheme, only post-flexure dykes are vertical

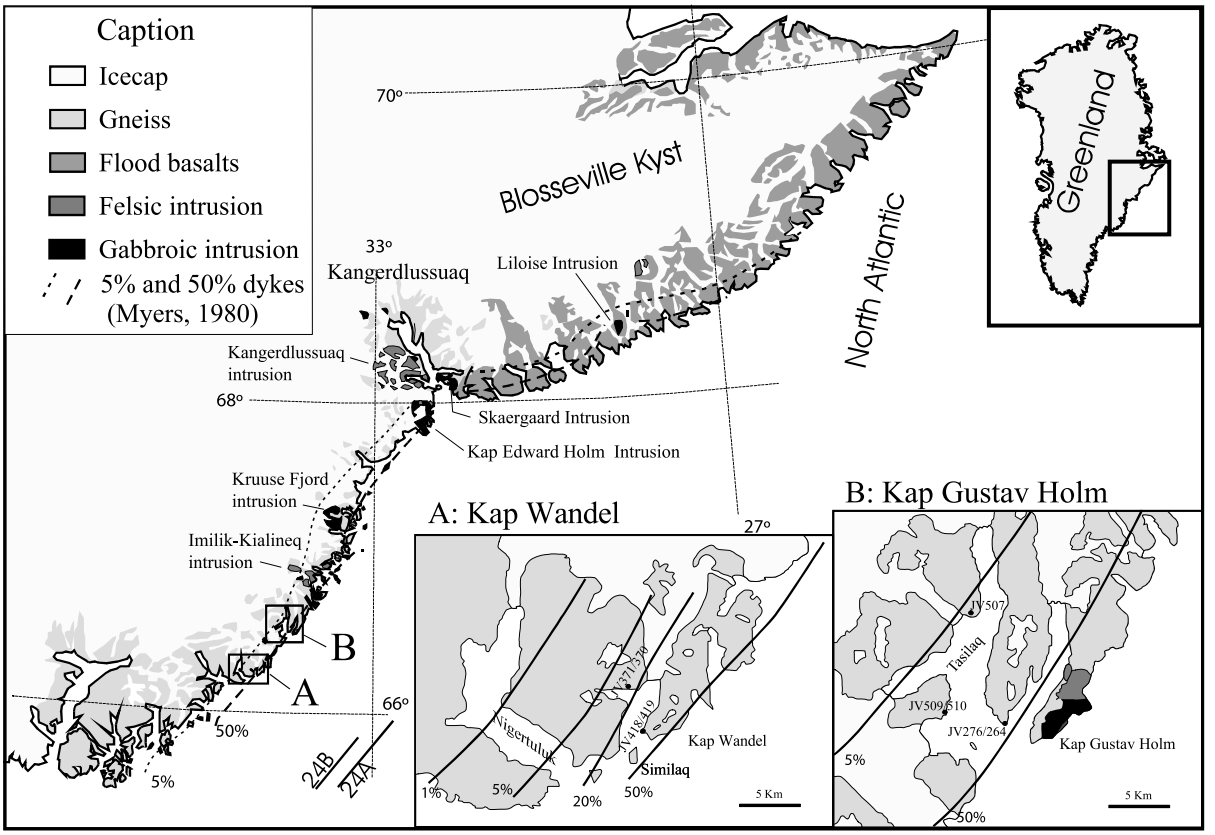

Fig. 2. Location of two sampling areas in the East Greenland volcanic margin. Insets, above: map of Greenland; below: maps of both study areas with location of sample pairs. In maps A and B, black lines correspond to contours (percent) of magmatic dilatation of the crust from dyke intrusion into the Precambrian crust [36].

(Fig. 3B). Several arguments support this assumption: (1) a roughly right angle between older tilted dykes and lowest tilted flows where dykes and lava flows are present [12,13,15,32], (2) very steep dipping of older dykes in areas where there is no evidence of Tertiary deformation [15] and (3) large post-cooling rotation of older dykes shown by some paleomagnetic data [35]. New paleomagnetic data on dykes from Kap Wandel and Kap Gustav Holm, which include some of the dated dykes, agree with a sub-vertical intrusion of preflexure or tilted dykes [36].

All dykes intrude a Precambrian basement of layered amphibolite gneiss. In both investigated localities, tilted dykes are generally thick (6–20 m) and have a doleritic texture whereas vertical dykes are thinner (< 5 m) and have a microdoleritic or microlitic porphyric texture. In both cases, the primary mineralogy is homogeneous with plagioclase (An_{40-70}), calcic augite, Fe–Ti oxides, scarce olivine and rare amphibole or biotite except for JV276 and JV264 where large amounts of Ti–Fe pargasite and biotite are present, respectively. Alteration affects all samples to various degrees. Plagioclases show various degrees of sericitization and olivine is generally replaced. Chlorite is a common secondary phase. Tilted and vertical dykes from Kap Wandel have tholeiitic and transitional to alkaline compositions, respectively. No similar feature was clearly established for dykes from Kap Gustav Holm [36].

On the basis of alteration criteria, we selected four dyke pairs among the freshest samples for $^{40}Ar/^{39}Ar$ dating (Fig. 2). Alteration affects all selected samples to various degrees, but the alteration of the analyzed minerals is detected by the

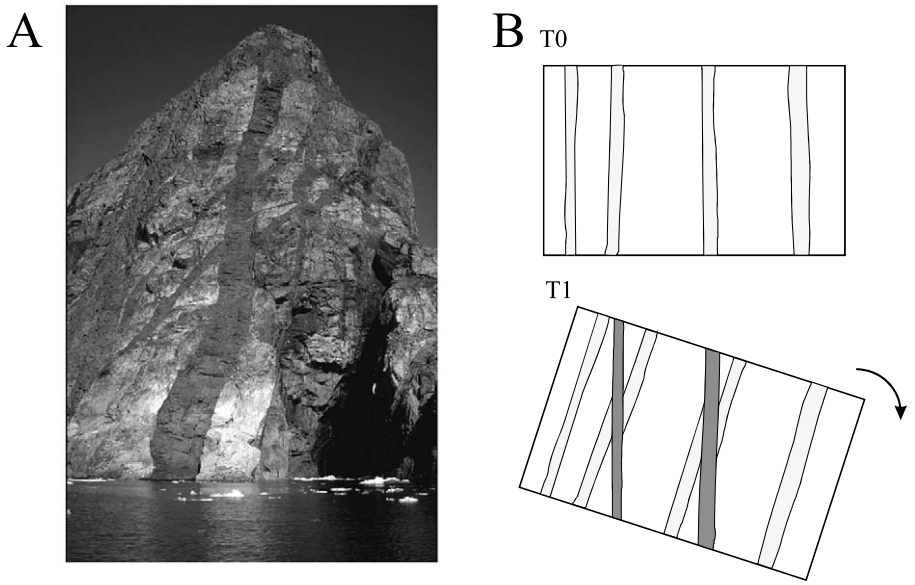

Fig. 3. (A) Photograph showing field relationship between distinct generations of dykes which progressively intruded the East Greenland volcanic margin during the flexure. (B) Schematic cartoon showing the relationship between dyke swarm structure and flexure. During progressive tilting of the margin, continuous intrusion of dykes reflects the evolution of the flexure. Dykes are assumed to have been initially intruded vertically and progressively tilted during the flexure.

$^{37}Ar_{Ca}/^{39}Ar_K$ ratio (see below). Plagioclase grains (100–200 μm fraction) were separated using a Frantz magnetic separator and carefully selected by hand-picking under a binocular microscope to prevent the presence of altered grains in mineral separates. Amphibole grains (250–400 μm fraction) and biotite grains were directly sampled out of crushed whole rocks. The weight of bulk samples ranges from 10 to 40 mg for plagioclase, and is about 40 mg and 2 mg for amphibole and biotite, respectively. The samples were irradiated in the nuclear reactor at McMaster University in Hamilton, ON, Canada, in position 5c. The total neutron flux density during irradiation was 8.82×10^{18} n/cm^2 except for JV370, where it was about 3.15×10^{18} n/cm^2. We used the HB3gr hornblende with an age of 1072 Ma [37] as a flux monitor, except for JV370 for which Fish Canyon sanidine at 28.02 Ma [38] was used. The bulk samples were step-heated with a double-vacuum high-frequency furnace directly connected to a 120°/12 cm M.A.S.S.E. mass spectrometer working with a Baür-Signer source and a Balzers SEV 217 electron multiplier. For a single grain of amphibole, gas extraction was carried out with a 50 W SYNRAD CO_2 continuous laser. Isotopic ratios were measured using a VG3600 mass spectrometer, working with a Daly detector system. The typical blank values for extraction and purification of the laser system are in the range 4.2–8.75, 1.2–3.9 and $0.3–0.5\times10^{-13}$ cc STP for masses 40, 39 and 36, respectively (measured every third step) whereas argon isotopes measured on the amphibole single grain were on the order of 16–1000, 20–1500 and 0.3–10 times blank level, respectively. Correction factors for interfering isotopes were $(^{39}Ar/^{37}Ar)_{Ca}=7.06\times10^{-4}$, $(^{36}Ar/^{37}Ar)_{Ca}=2.79\times10^{-4}$ and $(^{40}Ar/^{39}Ar)_K=2.97\times10^{-2}$. Decay constants are those of Steiger and Jäger [39]. Uncertainties on apparent ages are given at the 1σ level and do not include the error on the $^{40}Ar^*/^{39}Ar_K$ ratio of the monitor. Uncertainties on plateau and mini-plateau ages are given at the 2σ level and do not include the error on the age of the monitor.

4. $^{40}Ar/^{39}Ar$ results

The precise dating of dykes from the East

Table 3
Summarized $^{40}Ar/^{39}Ar$ data and general information for dated basaltic dykes of East Greenland

Sample	General information on dyke					Data of datings							Statistics on microprobe data		
	Location	Latitude	Longitude	Strike[a] dip	Thickness (m)	Material	Plateau age (Ma)	^{39}Ar (%)	Steps	Isochron age (Ma)	Initial $^{40}Ar/^{36}Ar$ ($\pm 1\sigma$)	MSWD	Grains	Core	Rim
JV370	Kap Wandel	66°20.5′	35°55′	013 90	17	Plagioclase	51.4 ± 0.7	23	6–8	46 ± 17	542 ± 800	0.9	14	16	14
JV371	Kap Wandel	66°20.5′	35°55′	032 65 N	5	Plagioclase	54.3 ± 2.2	54	7–14	52.8 ± 2.5	308 ± 16	0.5	12	27	13
JV418	Kap Wandel	66°18.9′	35°52.9′	022 69 N	2	Plagioclase	54.5 ± 1.9	39	7–11	54.4 ± 0.8	297 ± 16	0.01	14	29	15
JV419	Kap Wandel	66°18.9′	35°52.9′	015 90	9	Plagioclase	51.1 ± 1.4	50	9–17	43.8 ± 7.6	527 ± 226	0.4	12	22	12
JV264	Kap Gustav Holm	66°35.4′	34°24′	024 84 N	4	Biotite	51.0 ± 0.3	91	7–14	50.4 ± 0.4	295.8 ± 1.7	1.9			
JV276	Kap Gustav Holm	66°35.4′	34°24′	046 39 N	1	Amphibole	53.9 ± 0.6	84	13–20	52.2 ± 1.6	493 ± 203	0.4	12	18	12
JV509	Kap Gustav Holm	66°36.2′	34°30.4′	039 60 N	5	Plagioclase	54.7 ± 1.5	36	6–10	47.0 ± 11.8	487 ± 233	0.9	14	27	14
JV510	Kap Gustav Holm	66°36.2′	34°30.4′	045 90	0.8	Plagioclase	48.0 ± 2.8	50	7–11	50.4 ± 2.0	272 ± 15	0.8	15	29	18

[a] Uncertainties are given at 2σ except for the initial $^{40}Ar/^{36}Ar$ ratio of isochron (1σ).

Greenland margin is very difficult because of excess argon; all whole rock and plagioclase and amphibole separates show saddle-shaped age spectra. The excess argon is probably due to a contamination of the magma by the basement in which the dykes are intruded. Most of the rocks of the basement are probably strongly enriched in radiogenic ^{40}Ar as a result of radiogenic decay from potassium (Precambrian and K-rich rocks). In order to minimize the effect of excess argon, we performed very detailed age spectra on minerals that may allow differentiation between radiogenic argon (dominantly released at intermediate temperature) and argon in excess (mainly visible at low and high temperatures on saddle-shaped age spectra). In the case of no or a small amount of alteration phases, and several intermediate temperature steps giving concordant apparent ages, we may assume that the contribution of excess argon on this flat section of the spectrum is negligible and consequently that this 'mini-plateau age' is valid. Therefore, we have defined 'plateau or mini-plateau ages' with the following criteria: (1) at least three successive steps are included in the plateau age, (2) the integrated age of the plateau should agree with each apparent age of the plateau within a 2σ confidence interval. In this study, we do not define a minimum percentage of ^{39}Ar released for the plateau age (that is unusual for Ar/Ar geochronology), in order to approach the best estimate of the true age. Therefore, we may exclude some apparent ages on both sides of the mini-plateau age (that could be included in the plateau, if we strictly follow the criteria previously given), but that are clearly affected by excess argon (this is for instance the case for steps 6 and 12 of the plagioclase JV418, which we exclude from the accepted age).

Detailed and synthetic data are given in Tables 2[1] and 3, respectively. The inverse isochron data ($^{36}Ar/^{40}Ar$ vs. $^{39}Ar/^{40}Ar$) are also given in Table 3, but the diagrams are not shown. All data obtained on plagioclases are very clustered on these diagrams because of nearly similar atmospheric compositions, and consequently the initial $^{40}Ar/$

[1] See online version of this article.

^{36}Ar ratio is mostly poorly defined. Nevertheless, in some cases, we could verify that the initial ratio is atmospheric, and therefore that the selected mini-plateau ages are not affected by significant excess argon (JV371, 418, 510).

At Kap Gustav Holm (Fig. 2), two pairs of dykes were investigated. The ages of the first pair (JV509 and JV510) were measured on plagioclase bulk samples. Both samples display saddle-shaped age spectra characterized by discordant mini-plateau ages of 54.7 ± 1.5 Ma for the tilted dyke (JV509) and 48.0 ± 2.8 Ma for the vertical dyke (JV510) corresponding to 36 and 50% of the total ^{39}Ar released, respectively (Fig. 4). The Ca/K ratio of JV510, which is proportional to the ratio $^{37}Ar_{Ca}/^{39}Ar_K$ (with the relationship $Ca/K = 1.83 \times {}^{37}Ar_{Ca}/^{39}Ar_K$) is not constant on the plateau fraction (between 12.4 and 31.5), but is in good agreement with Ca/K ratios which are measured on plagioclase with the microprobe (boxplots in Fig. 4). This shows that the $^{37}Ar_{Ca}/^{39}Ar_K$ variations in the plateau fraction probably correspond to nearly pure plagioclases. JV509 displays a constant $^{37}Ar_{Ca}/^{39}Ar_K$ ratio on the plateau fraction, which corresponds to similar Ca/K ratios obtained with the microprobe, and therefore to pure plagioclase. For the second pair, the amphibole single grain from the tilted dyke (JV276) provides a plateau age of 53.9 ± 0.6 Ma for 84% of the total ^{39}Ar released, with a slight excess argon restricted to the lowest temperature steps. The bulk sample of amphibole shows a saddle-shaped age spectrum with a minimum apparent age of 54.2 ± 0.3 Ma, concordant with the single-grain plateau age. In both cases, the analyzed amphibole corresponds to a pure mineral as shown by the corresponding $^{37}Ar_{Ca}/^{39}Ar_K$ ratio spectrum (Fig. 4). The presence of higher excess argon in the bulk sample may indicate that the excess is not homogeneously distributed in the amphibole population. The biotite bulk sample from the vertical dyke (JV264) displays a significantly younger plateau age of 51.0 ± 0.3 Ma for 91% of the total

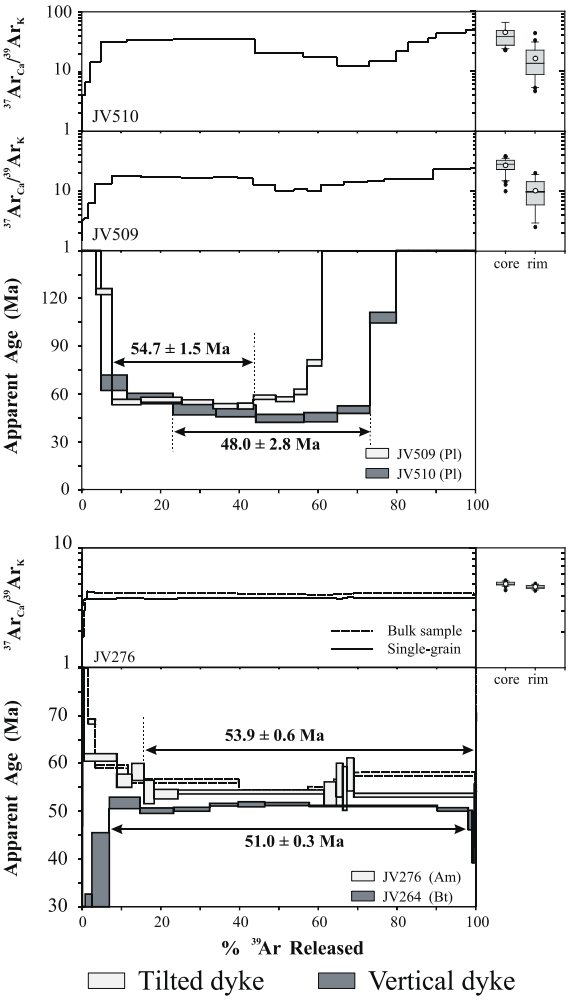

Fig. 4. Detailed ^{40}Ar/^{39}Ar age and $^{37}Ar_{Ca}/^{39}Ar_K$ ratio spectra obtained on mineral separates from dyke pairs of Kap Gustav Holm, East Greenland (see Fig. 2). Uncertainties on apparent ages are given at the 1σ level, whereas uncertainties on plateau and mini-plateau ages are given at the 2σ level. Tilted and vertical dykes are in light and dark gray, respectively. All dating was performed on mineral bulk samples except for JV276 for which one single grain of amphibole was used. To compare with $^{37}Ar_{Ca}/^{39}Ar_K$ ratio spectra, boxplots of $^{37}Ar_{Ca}/^{39}Ar_K$ ratios, which were calculated from microprobe analysis, are also shown. The box depicts the central part of the analysis distribution, roughly between the 25th and 75th percentiles. The line across the box displays the median value of the distribution. Lines extending from the box represent the range of observed values between the 10th and 90th percentiles. Open and closed circles correspond to mean of analysis distribution and individual analysis outside these distribution boundaries, respectively (see Table 3 for statistical information). The sizes of microprobe-analyzed grains are representative of dated mineral grain size. Am: amphibole, Bt: biotite; Pl: plagioclase.

^{39}Ar released. A slight chloritization of the analyzed biotite is possible (but not demonstrated) as shown by the increase of apparent age at low temperature (< 6% of the total ^{39}Ar released) but it should not affect the plateau age. The isochron plot displays a concordant age of 50.4 ± 0.4 Ma and an atmospheric initial ^{40}Ar/^{36}Ar ratio of 295.8 ± 1.5 (MSWD = 1.9).

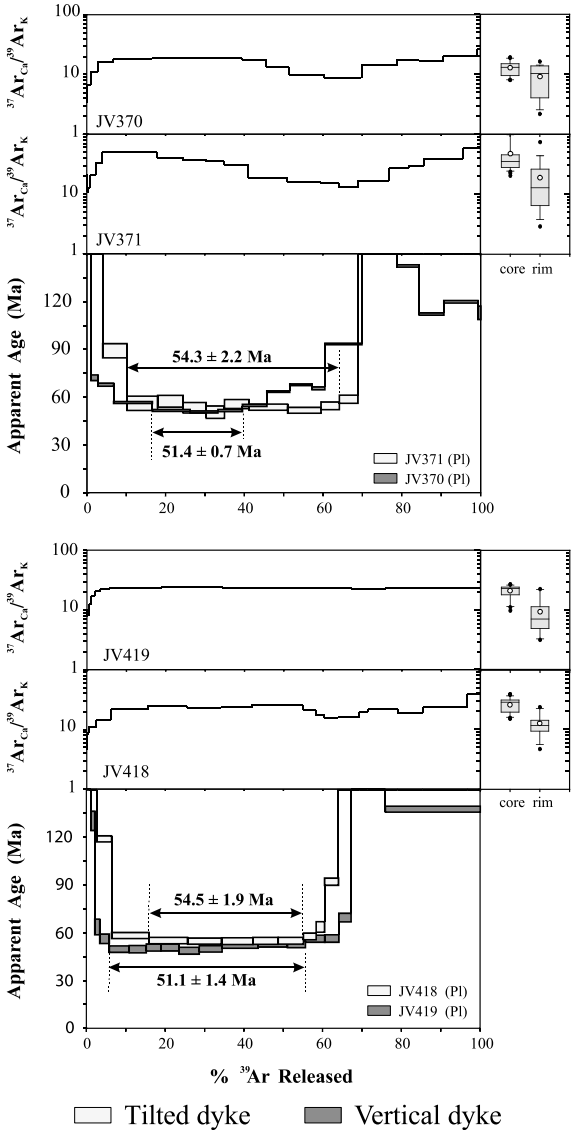

Fig. 5. Detailed ^{40}Ar/^{39}Ar ages and $^{37}Ar_{Ca}/^{39}Ar_K$ ratio spectra obtained on mineral separates from dyke pairs of Kap Wandel, East Greenland (see Fig. 2). Legend as for Fig. 4.

On dykes from Kap Wandel, all ages were measured on plagioclase bulk samples. For the first dyke pair, age spectra display mini-plateau ages at 54.3 ± 2.2 Ma for the tilted dyke (JV371) and 51.4 ± 0.7 Ma for the vertical dyke (JV370) corresponding to 54% and 23% of the total ^{39}Ar released, respectively (Fig. 5). Sample JV371 shows a moderate variation of the $^{37}Ar_{Ca}/^{39}Ar_K$ ratio on the plateau fraction, but any effect of alteration is probably low because of the agreement between microprobe and isotopic determinations of Ca/K ratios (Fig. 5). For sample JV370, the plateau fraction corresponds to the highest and flat part of the $^{37}Ar_{Ca}/^{39}Ar_K$ ratio spectrum. For the second dyke pair, tilted (JV418) and vertical (JV419) dykes show remarkably similar age spectra with mini-plateau ages of 54.5 ± 1.9 Ma over 39% of ^{39}Ar released and 51.1 ± 1.4 Ma over 50% of ^{39}Ar released, respectively (Fig. 5). In both cases, the regularity of the $^{37}Ar_{Ca}/^{39}Ar_K$ ratio spectra demonstrates the high purity of the analyzed grains (Fig. 5).

5. Discussion and conclusion

5.1. Bracketing in age the coastal flexure

All the plagioclase grains display saddle-shaped age spectra, demonstrating the existence of excess argon. Amphibole (laser experiment) and biotite from one pair of dykes from Kap Gustav Holm display plateau ages defining an age difference of 2.9 Ma (between 2.0 and 3.8 Ma when we take into account the errors) between the emplacement of the tilted and the vertical dykes. When we examine the previously mentioned 'mini-plateau ages' displayed by plagioclase age spectra, we systematically observe an older age for the tilted dykes. Moreover, (1) the tilted dykes give concordant mini-plateau ages (54.3 ± 2.2, 54.5 ± 1.9 and 54.7 ± 1.5) in agreement with the amphibole plateau age of 53.9 ± 0.6 Ma, and (2) the vertical dykes give concordant mini-plateau ages (51.4 ± 0.7, 51.1 ± 1.4 and 48.8 ± 2.8 Ma) in agreement with the biotite plateau age of 51.0 ± 0.3 Ma.

All the isochron ages are concordant with pla-

teau and mini-plateau ages, but the clustering of data on plagioclases on these diagrams does not make it possible to provide useful information on the ages. Nevertheless, and despite their large errors, the initial $^{40}Ar/^{36}Ar$ ratios do not show evidence of significant excess argon that could induce too high ages on the selected gas fractions. Consequently, and although these minimum intermediate temperature ages (calculated on more or less low gas fractions) strictly represent minimum ages, because of: (1) the flatness of the mini-plateaus, (2) the concordance of data on plagioclase, biotite and amphibole obtained on the same family of dykes (vertical or tilted) and (3) the absence of evidenced excess argon (from the best defined initial $^{40}Ar/^{36}Ar$ ratios), they probably represent reasonable estimates of the age of emplacement of these dykes. Such a conclusion was previously suggested by Deckart et al. [40] for plagioclases from dykes affected by excess argon. Moreover, we have seen that alteration phases are nearly absent on the corresponding gas fractions, as shown by the $^{37}Ar_{Ca}/^{39}Ar_K$ ratio.

Fig. 6 shows age differences (without taking into account errors) between tilted and vertical ages ranging from 2.9 to 6.7 Ma, and probably more realistic values on the order of 2.9 Ma displayed by the more precise amphibole and biotite plateau ages. Finally, these measured ages of tilted and vertical dykes are in good agreement with recently published $^{40}Ar/^{39}Ar$ ages on mafic intrusions, onshore flood basalts and SDRS (Table 1). Ages of tilted and vertical dykes could correspond to the second (54–57 Ma) and third (50–47 Ma) pulses of tholeiitic magmatism proposed by Tegner et al. [27], respectively.

So, two generations of dykes at Kap Wandel and Kap Gustav Holm are identified: (1) a tilted swarm at 54–55 Ma and (2) a vertical swarm at around 51 Ma (Fig. 6). To estimate the true significance of this time span, several features must be taken into account, such as strikes of dykes in comparison with the presumed axis of flexure, initial (post-injection) dip of tilted dykes and delay time between injection of early dykes and development of the flexure.

At Kap Wandel, average strikes of dykes range from N38°E to 30°E and from N38°E to N19°E

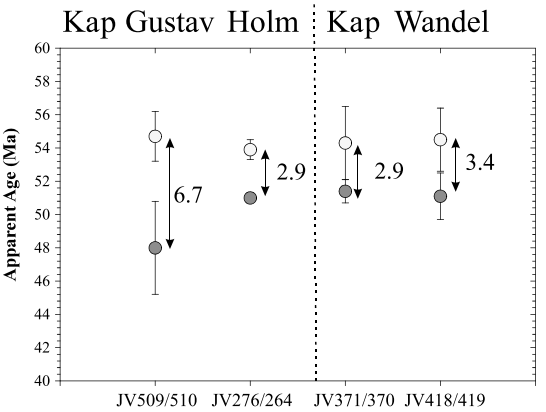

Fig. 6. Systematic age difference between tilted and vertical dykes. Light and dark gray circles correspond to tilted and vertical dykes, respectively. Uncertainties on ages are given at the 2σ level.

for tilted and vertical dykes, respectively. At Kap Gustav Holm, they range from N44°E to N27°E without possible trend distinction between the two generations of dykes [31,36]. Strikes of dated dykes generally agree with these features (see Table 3). Tilted dykes in first approximation keep similar trends whereas their dips vary considerably with values ranging from 80° to 60°NW, and from 80° to 40°NW at Kap Wandel and Kap Gustav Holm, respectively [31,36]. It appears therefore that the presumed axis of flexure must be comparable to the constant average strike of tilted dykes which, probably, injected throughout the margin flexing (see also [41]). Therefore, the dip of dykes as a result of flexing was not significantly affected by their injection strike.

In the two studied areas, all the observable east-dipping dykes (280 intrusions) were geometrically cross-cut by vertical or sub-vertical dykes. Along the whole CDS, the vertical dykes form a distinct set from the others not only from their dip but also from their chemistry [34,36]. It appears evident that the vertical attitude of these transitional to alkaline-type ubiquitous dykes is inherited from their injection and that they therefore clearly postdate the flexing of the crust. One may consider the hypothesis that some, at least, of the tilted dykes could have been injected obliquely. Taking dykes as mode-I intrusions, this

could be a consequence of oblique principal stresses during crustal flexure [42]. Alternatively, considering the principal stresses as vertical and horizontal, a possible mixed-mode tension-shear injection may also be invoked in inherited fractures [43] or even as newly formed intrusions [44]. In this latter case, one could expect some 'conjugated' dykes (i.e. eastward-dipping), a feature that we did not observe along the CDS sections that we investigated. No field observations support the former case in the studied areas. The assumption that tilted dykes were non-vertical dykes when they were injected is thus far the harder to defend and anyway does not explain the progressive incremental tilt of this tholeiite-type generation.

Because the sampled titled dykes display the most gentle dip, it is likely that these dykes intruded the crust prior to or just at the beginning of the coastal flexure. Likewise, vertical dykes probably intruded the crust after the flexure because they are apparently not affected by any tilting related to the flexing. A delay time between the end of flexing and intrusions of vertical dykes may exist. Therefore, our estimation of flexure duration must be considered as a maximum value, and the flexure of the East Greenland margin developed between 54 Ma and 51 Ma with a maximum duration of about 2.9 Ma (2.0–3.8 Ma with errors). This time interval is larger than that which is proposed by Schwarz et al. [28], about 250 kyr. However, our time interval is strongly constrained by datings contrary to Schwarz et al. [28]. Our estimation of the lower and upper limits of flexure age seems reliable because: (1) recent $^{40}Ar/^{39}Ar$ ages obtained on the tilted intrusion of Skaergaard imply that the onset of flexure was after 55.5 ± 0.76 Ma [25]; (2) the end of flexing occurred before ~ 50 Ma as a result of K–Ar (51 ± 2 Ma) and Rb–Sr (50 ± 3 Ma) mineral ages obtained on biotites from granite and monzonite plutons in the Kap Gustav Holm center which are apparently not tilted [45].

5.2. *Evaluation of the crustal extension rate at the East Greenland VPM*

In a VPM, the full finite horizontal extension of the crust should be determined by the sum of: (1) crustal stretching through ductile boudinage and normal faulting and (2) magmatic dilatation resulting from the intrusion of dykes. Unfortunately, the amount of tectonic stretching by faults is poorly known at the VPM of East Greenland around the studied area. Nevertheless, a quantitative estimation of tectonic extension could be simply given using a pure-shear model for lithospheric deformation. In this scheme, the percentage of tectonic extension could be evaluated by the ratio between the thickness of thinned crust along the VPM and normal crust taken outside the VPM (e.g. [46,47]).

On the basis of seismic line 2 from the Sigma experiment [8] and a P-wave velocity up to 7.0 km/s for the lower continental crust – whereas the underplated igneous crust presents a P-wave velocity ranging from 7.2 to 7.5 km/s [48] – the thinned crust has presently a thickness of about 25 km in the study area. The reference thickness of the unstretched crust beneath Greenland is unknown. However, the extremity of seismic line 2 [8] used some land seismometers. The calculated thickness of the crust increases up to 29 km continentward 50 km from the coastline taking a velocity of 7.0 km/s for the continental crust. This indicates that the β factor of crustal thinning along the coast would reach a minimal value of 1.14, i.e. 14% tectonic extension.

The magmatic dilatation is evaluated from the ratio between the sum of thickness – considering both strike and dip – of dikes and the length of the cross-section for the inner, middle and outer parts of the margin. A value of 50% for magmatic dilatation is calculated at the emplacement of dykes in accordance with both our field determinations and the published map of magmatic dilatation [49]. Note that crustal dilatation by dyking has no major effect on crustal thinning contrary to crustal extension through faulting/flexing in the upper crust and ductile flow in the lower crust.

Therefore, the full finite horizontal extension along this part of the coastline of East Greenland could be estimated to be up to 64% providing a strain rate value of 7×10^{-15} s^{-1}. The propagation of age uncertainties for flexure duration on strain

rate calculation gives an uncertainty of 2×10^{-15} s^{-1}. It should be noted that uncertainties on the crust thickness have a smaller effect than uncertainties on ages, as an uncertainty of 2 km on both the thickness of pre-rift and actual crust gives an error of only 0.5×10^{-15} s^{-1}.

The calculated strain rate value is very high but it constitutes a lower limit. The true value of strain rate must indeed be significantly higher considering that the time interval between pre-flexure and post-flexure dykes of 2.9 (2.0–3.8 Ma with errors) Ma is a maximum (see above). In addition, provided the thickness of the continental crust beneath the Inlandsis is higher than 29 km (such is the case north of Scoreby Sund where it is up to 47 km [50]), this also considerably increases this value of strain rate. We thus demonstrate that strain rates are very high at VPMs compared to strain rates of intracontinental rift basins or non-VPMs which range from 10^{-17} to 10^{-15} s^{-1} [51] and 10^{-16} to 6×10^{-15} s^{-1} [52], respectively. Such high strain rates could be linked with the occurrence of Tertiary pseudotachylytes in East Greenland [17] but pseudotachylytes form at much higher strain rates and relate to different time-scale phenomena (seismic faulting, e.g. [53]). Our results are in agreement with the evidence for a short-term tilting of Skaergaard intrusion [28].

This high strain rate could be interpreted as resulting from high thermal flux at VPMs. Indeed, high thermal flux is thought to lead to a localized weakening of the lithosphere and narrowing of the deformation zone in the lithosphere (e.g. [54]). Crustal thinning is clearly imaged at VPMs (e.g. [8,48,55]). On the other hand, the duration of the rifting stage at non-volcanic rifts and passive margins ranges from 14 to 275 Ma [56]. Even if the 2.0–3.8 Ma time span calculated in the studied area may not reflect the whole duration of extension along the East Greenland rift (oceanward rift jumps may have occurred) the duration of the rifting stage seems significantly lower (one or two orders) at VPMs compared to non-volcanic break-up areas. All these data lead to the suggestion that the lithospheric break-up above a mantle plume is a 'catastrophic' phenomenon as previously suggested by Hinz [5].

Acknowledgements

We thank Jeff Karson and an anonymous reviewer for constructive reviews of the manuscript. The research work was financed by the GDR Marges (contribution no. 22) and Géosciences Azur (contribution no. 577). Financial and logistical support for the field trip on the East Greenland coast came from IFRTP and the GDR Marges. *[KF]*

References

[1] O. Eldholm, J. Skogseid, S. Planke, T.P. Gladczenko, Volcanic margins concept, in: E. Banda et al. (Eds.), Rifted Ocean-Continent Boundaries, NATO ASI Series, Kluwer Academic, Dordrecht, 1995, pp. 1–16.
[2] R. White, D. McKenzie, Magmatism at rift zones: The generation of volcanic continental margins and flood basalts, J. Geophys. Res. 94 (1989) 7685–7729.
[3] V. Courtillot, C. Jaupart, I. Manighetti, P. Tapponnier, J. Besse, On causal links between flood basalts and continental breakup, Earth Planet. Sci. Lett. 166 (1999) 177–195.
[4] A.K. Pedersen, M. Watt, W.S. Watt, L.M. Larsen, Structure and stratigraphy of the Early Tertiary basalts of the Blosseville Kyst, East Greenland, J. Geol. Soc. London 154 (1997) 565–570.
[5] K. Hinz, A hypothesis on terrestrial catastrophes: Wedges of very thick oceanward dipping layers beneath passive continental margins – their origin and paleoenvironmental significance, Geol. Jahrb. R. Geophys. 22 (1981) 3–28.
[6] L. Geoffroy, J.P. Gelard, C. Lepvrier, P. Olivier, The coastal flexure of Disko (West Greenland), onshore expression of the 'oblique reflectors', J. Geol. Soc. London 155 (1998) 463–473.
[7] L. Geoffroy, The structure of volcanic margins some problematics from the North-Atlantic/Labrador-Baffin system, Mar. Pet. Geol. 18 (2001) 463–469.
[8] W.S. Holbrook, H.C. Larsen, J. Korenaga, T. Dahl-Jensen, I.D. Reid, P.B. Kelemen, J.R. Hopper, G.M. Kent, D. Lizarralde, S. Bernstein, R.S. Detrick, Mantle structure and active upwelling during continental breakup in the North Atlantic, Earth Planet. Sci. Lett. 190 (2001) 251–266.
[9] D.L. Anderson, The sublithosperic mantle as the source of continental flood basalts; the case against the continental lithosphere and plume head reservoirs, Earth Planet. Sci. Lett. 123 (1994) 269–280.
[10] W.S. Holbrook, P.B. Kelemen, Large igneous province on the United States Atlantic margin and implications for magmatism during break-up, Nature 364 (1993) 433–436.
[11] M. Wilson, Thermal evolution of the Central Atlantic

passive margins: continental break-up above a Mesozoic super-plume, J. Geol. Soc. London 154 (1997) 491–495.
[12] T.F.D. Nielsen, Possible mechanism of continental break-up in the North Atlantic, Nature 253 (1975) 182–184.
[13] J.S. Myers, Structure of the coastal dyke swarm and associated plutonic intrusions of East Greenland, Earth Planet. Sci. Lett. 46 (1980) 407–418.
[14] T.F.D. Nielsen, C.K. Brooks, The E Greenland rifted continental margin: an examination of the coastal flexure, J. Geol. Soc. London 138 (1981) 559–568.
[15] J.A. Karson, C.K. Brooks, Structural and magmatic segmentation of the Tertiary East Greenland Volcanic Rifted Margin, in: C. Mac Niocaill, P.D. Ryan (Eds.), Continental Tectonics, Geol. Soc. London Spec. Publ. 164 (1999) 313–338.
[16] G. Palmason, A continuum model of crustal generation in Iceland kinematic aspects, J. Geophys. 47 (1980) 7–18.
[17] J.A. Karson, C.K. Brooks, M. Storey, M. Pringle, Tertiary faulting and pseudotachylytes in the East Greenland volcanic rifted margin: Seismogenic faulting during magmatic construction, Geology 26 (1998) 39–42.
[18] P. Japsen, J.A. Chalmers, Neogene uplift and tectonics around the North Atlantic: overview, Global Planet. Change 24 (2000) 165–173.
[19] M.H.P. Bott, The continental margin of central East Greenland in relation to North Atlantic plate tectonic evolution, J. Geol. Soc. London 144 (1987) 561–568.
[20] R.H. Noble, R.M. Macintyre, P.E. Brown, Age constraints on Atlantic evolution: timing of magmatic along the E Greenland continental margin, in: A.C. Morton, L.M. Parson (Eds.), Early Tertiary Volcanism and the opening of the NE Atlantic, Geol. Soc. London Spec. Publ. 39 (1988) 201–214.
[21] H. Hansen, D.C. Rex, P.G. Guise, C.K. Brooks, ^{40}Ar-^{39}Ar ages on early Tertiary basalts from the Scoresby Sund area, East Greenland, Newsl. Stratigr. 32 (1995) 103–116.
[22] C.W. Sinton, R.A. Duncan, ^{40}Ar-^{39}Ar ages of lavas from the southeast Greenland margin, ODP leg 152, and the Rockall plateau, DSDP leg 181, in: A.D. Saunders, H.C. Larsen, S.W. Wise, Jr. (Eds.), Proc. ODP Sci. Results 152 (1998) 387–402.
[23] M. Storey, R.A. Duncan, H.C. Larsen, A.K. Pedersen, R. Waagstein, L.M. Larsen, C. Tegner, C.E. Lesher, Impact and rapid flow of the Iceland plume beneath Greenland at 61 Ma, EOS Trans. AGU Fall Meet. Suppl. 77, 1996, p. 839.
[24] C. Tegner, R.A. Duncan, ^{40}Ar-^{39}Ar chronology for the volcanic history of the southeast Greenland rifted margin, in: H.C. Larsen, R.A. Duncan, J.F. Allan, K. Brooks (Eds.), Proc. ODP Sci. Results 163 (1999) 53–62.
[25] M.M. Hirsmann, P.R. Renne, A.R. McBirney, ^{40}Ar-^{39}Ar dating of the Skaergaard intrusion, Earth Planet. Sci. Lett. 146 (1997) 645–658.
[26] R.J. Nevle, M.E. Brandriss, M.O. McWilliams, J.R. O'Neill, Tertiary plutons monitor climate change in East Greenland, Geology 22 (1994) 775–778.
[27] C. Tegner, R.A. Duncan, S. Bernstein, C.K. Brooks, D.K. Bird, M. Storey, ^{40}Ar-^{39}Ar geochronology of Tertiary mafic intrusions along the East Greenland rifted margin: Relations to flood basalts and the Iceland hotspot track, Earth Planet. Sci. Lett. 156 (1998) 75–88.
[28] E.J. Schwarz, L.C. Coleman, H.M. Cattroll, Paleomagnetic results from the Skaergaard intrusion, East Greenland, Earth Planet. Sci. Lett. 42 (1979) 437–443.
[29] K. Hansen, Tracking thermal history in East Greenland: an overview, Global Planet. Change 24 (2000) 303–309.
[30] C.K. Brooks, Rifting and doming in southern East Greenland, Nature 244 (1973) 23–25.
[31] M. Bromann-Klausen, H.C. Larsen, East Greenland coast-parallel dike swarm and its role in continental breakup, in: M.A. Menzies, S.L. Klemperer, C.J. Ebinger, J. Baker (Eds.), Volcanic Rifted Margins, GSA Spec. Pap. 362 (2002) 133–158.
[32] T.F.D. Nielsen, The Tertiary dike swarm of the Kangerlugssuaq area, East Greenland. An example of magmatic development during continental break-up, Contrib. Mineral. Petrol. 67 (1978) 63–78.
[33] R.C.O. Gill, T.F.D. Nielsen, C.K. Brooks, G.A. Ingram, Tertiary volcanism in the Kangerdlugssuaq region, E Greenland: trace-element geochemistry of the Lower Basalts and tholeiitic dyke swarms, in: A.C. Morton, L.M. Parson (Eds.), Early Tertiary Volcanism and the Opening of the NE Atlantic, Geol. Soc. London Spec. Publ. 39 (1988) 161–179.
[34] K. Hanghoj, M. Storey, O. Stecher, An isotope and trace element study of the East Greenland Tertiary dyke swarm: Constraints on temporal and spatial evolution during continental rifting, J. Petrol. (in press).
[35] L.D. Guenther, K.L. Verosun, S.D. Hurst, J.A. Karson, Paleomagnetic constraints on the evolution of the Tertiary East Greenland coast-parallel dike swarm: tectonics rotations at a volcanic rifted margin, EOS Trans. AGU 77 (1996) 824.
[36] J.-P. Callot, Origine, structure et développement des marges volcaniques: l'exemple du Groenland, Unpublished Phd Thesis, Université de Paris VI, Paris, 2002, 430 pp.
[37] G. Turner, J.C. Huneke, F.A. Podose, G.J. Wasserburg, ^{40}Ar-^{39}Ar ages and cosmic ray exposure ages of Apollo 14 samples, Earth Planet. Sci. Lett. 12 (1971) 19–35.
[38] P.R. Renne, C.C. Swisher, A.L. Deino, D.B. Karner, T. Owens, D.J. De Paolo, Intercalibration of standards, absolute ages and uncertainties in ^{40}Ar/^{39}Ar dating, Chem. Geol. Isotope Geosci. Sect. 145 (1998) 117–152.
[39] R.H. Steiger, E. Jäger, Subcommission on geochronology: convention of the use of decay constants in geo- and cosmochronology, Earth Planet. Sci. Lett. 36 (1977) 359–362.
[40] K. Deckart, G. Féraud, H. Bertrand, Age of Jurassic continental tholeiites of French Guyana/Surinam and Guinea: Implications to the initial opening of Central Atlantic Ocean, Earth Planet. Sci. Lett. 150 (1997) 205–220.

[41] L. Geoffroy, J.-P. Callot, S. Scaillet, A. Skuce, J.P. Gélard, M. Ravilly, J. Angelier, B. Bonin, C. Cayet, K. Perrot, C. Lepvrier, Southeast Baffin volcanic margin and the North American-Greenland plate separation, Tectonics 20 (2001) 566–584.
[42] W. Hafner, Stress distribution and faulting, Geol. Soc. Am. Bull. 62 (1951) 373–398.
[43] P.T. Delaney, D.D. Pollard, J.L. Ziony, E.H. McKee, Field relations between dikes and joints: emplacement processes and paleostress analysis, J. Geophys. Res. 91 (1986) 4920–4938.
[44] L. Geoffroy, J. Angelier, Mise en évidence de dykes en tension-cisaillement: définition et interprétation mécanique, C.R. Acad. Sci. Paris 321 (1995) 505–511.
[45] J.S. Myers, R.C.O. Gill, D.C. Rex, N.R. Charnley, The Kap Gustav Holm tertiary plutonic centre, East Greenland, J. Geol. Soc. London 150 (1993) 259–276.
[46] D. McKenzie, Some remarks on the development of sedimentary basins, Earth Planet. Sci. Lett. 40 (1978) 25–32.
[47] X. Le Pichon, J.C. Sibuet, Passive margin: A model of formation, J. Geophys. Res. 86 (1981) 3708–3720.
[48] J. Korenaga, W.S. Holbrook, G.M. Kent, P.B. Kelemen, R.S. Detrick, H.C. Larsen, J.R. Hopper, T. Dahl-Jensen, Crustal structure of the southeast Greenland margin from joint refraction and reflection seismic tomography, J. Geophys. Res. 105 (2000) 21591–21614.
[49] J.S. Myers, P.R. Dawes, T.F.D. Nieslsen, Geological Map of Greenland, Sheet 13: Kangerdlugssuaq, Geological Survey of Greenland and Geodetic Institute of Denmark, Copenhagen, 1988.
[50] V. Schlindwein, Architecture and evolution of the continental crust of East Greenland from integrated geophysical studies, Reports Polar Res. 270 (1998) 148 pp.
[51] R. Newman, N.J. White, Rheology of the continental lithosphere inferred from sedimentary basins, Nature 385 (1987) 621–624.
[52] M. Davis, N. Kusznir, Are buoyancy forces important during the formation or rifted margins?, Geophys. J. Int. 149 (2002) 524–533.
[53] R.H. Sibson, Generation of pseudotachylyte by ancient seismic faulting, Geophys. J. R. Astron. Soc. 43 (1975) 775–794.
[54] N.J. Kusznir, R.G. Park, The extensional strength of the continental lithosphere: its dependence on geothermal gradient, and crustal composition and thickness, in: M.P. Coward, J.F. Dewey, P.L. Hancock (Eds.), Continental Extensional Tectonism, Geol. Soc. London Spec. Pap. 28 (1987) 35–52.
[55] R.S. White, G.D. Spence, S.R. Fowler, D.P. McKenzie, G.K. Westbrook, A.N. Bowen, Magmatism at rifted continental margins, Nature 330 (1987) 439–444.
[56] P.A. Ziegler, Geodynamic processes governing development of rifted basins, in: F. Roure, N. Ellouz, V.S. Schein, I. Skvortsov (Eds.), Geodynamic Evolution of Sedimentary Basins, International Symposium, Moscow, 1994, pp. 19–67.
[57] H.C. Larsen, A.D. Saunders, Tectonism and volcanism at the southeast Greenland rifted margin: a record of plume impact and later continental rupture, in: A.D. Saunders, H.C. Larsen, S.W. Wise, Jr. (Eds.), Proc. ODP Sci. Results 152 (1998) 503–533.